

# Concept-based Explanations for Out-Of-Distribution Detectors

Jihye Choi <sup>1</sup>, Jayaram Raghuram <sup>1</sup>, Ryan Feng <sup>2</sup>, Jiefeng Chen <sup>1</sup>, Somesh Jha <sup>1</sup>, Atul Prakash <sup>2</sup>

<sup>1</sup> University of Wisconsin - Madison <sup>2</sup> University of Michigan

{jihye, jayaramr, jiefeng, jha}@cs.wisc.edu

{rtfeng, aprakash}@umich.edu

## ABSTRACT

Out-of-distribution (OOD) detection plays a crucial role in ensuring the safe deployment of deep neural network (DNN) classifiers. While a myriad of methods have focused on improving the performance of OOD detectors, a critical gap remains in interpreting their decisions. We help bridge this gap by providing explanations for OOD detectors based on learned high-level concepts. We first propose two new metrics for assessing the effectiveness of a particular set of concepts for explaining OOD detectors: 1) *detection completeness*, which quantifies the sufficiency of concepts for explaining an OOD-detector’s decisions, and 2) *concept separability*, which captures the distributional separation between in-distribution and OOD data in the concept space. Based on these metrics, we propose a framework for learning a set of concepts that satisfy the desired properties of detection completeness and concept separability and demonstrate the framework’s effectiveness in providing concept-based explanations for diverse OOD techniques. We also show how to identify prominent concepts that contribute to the detection results via a modified Shapley value-based importance score.

## 1 Introduction

It is well known that a machine learning (ML) model can yield uncertain and unreliable predictions on OOD inputs from an unknown distribution on which the model was not trained [1, 2, 3]. The most common line of defense in this situation is to augment the ML model (*e.g.*, a DNN classifier) with a detector that can identify and flag such inputs as being OOD. The ML model can then abstain from making predictions on such inputs [4, 5, 6]. Being a statistical model, any OOD detector makes incorrect decisions, *i.e.*, identifies in-distribution (ID) inputs as OOD and vice-versa. For instance, an OOD detector paired with a medical-diagnosis model may consistently detect a specific type of OOD input as ID, although the input may be clearly OOD to a human analyst. Such errors by an OOD detector without explanations can reduce the trust of a human analyst in the detector’s predictions, thereby limiting the broad adoption of OOD detectors in real systems.

Recently, the problem of learning OOD detectors with better performance is receiving increased attention [7, 6, 5, 8]. However, the related problem of explaining the decisions of an OOD detector has remained largely unexplored. Naturally, one may consider running an existing interpretation (attribution) method for DNN classifiers with in-distribution and OOD data separately, and then inspecting the difference between the two generated explanations. Unfortunately, there is no guarantee that an explanation method that can successfully explain class predictions can also be effective for OOD detectors. For instance, feature attributions, the most popular type of explanation [9, 10], may not capture visual difference in the generated explanations between ID and OOD inputs [11]. Moreover, their explanations based on pixel-level activations may not provide the most intuitive form of explanations for humans. On the other hand, concept-based explanations [12, 13, 14, 15] are another class of explanation methods that aims to reason about the behavior of DNN classifiers in terms of high-level concepts that are more intuitive to humans. However, the use of concept-based explanations for OOD detectors still remains unexplored.

In this paper, we seek to address the above technical gap. Our main contribution is, to our knowledge, the first method to help interpret the decisions of an OOD detector in terms of *high-level concepts*. For instance, Fig. 1 illustrates a concept-based explanation of two inputs, both of which are classified as Zebra by a DNN classifier, but one is detected as ID and the other is detected as OOD by an OOD detector. The high-level concepts in this example are whether an image contains stripes, oval face, sky, or greenery. However, a research question is *how can one determine a good set of concepts that are appropriate to reason about why an OOD detector determines a certain input to be ID or OOD?* To this end, we make the following contributions:

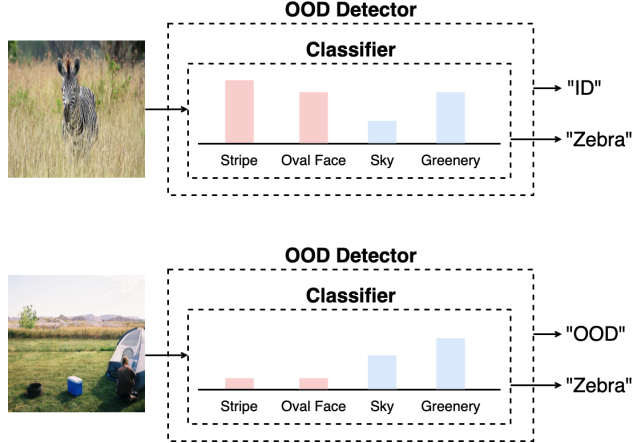


Figure 1: **Concept-based explanation for OOD detector.** "Stripe", "Oval Face", "Sky" and "Greenery" are concepts that completely explain the behavior of the classifier and OOD detector. Even though their class predictions are the same, OOD-detected input may have very different concept patterns compared to that of ID-detected input.

- We propose metrics to quantify the effectiveness of concept-based explanation for OOD detection: *detection completeness* and *concept separability* (§ 2.2, § 3.1, and § 3.2).
- We introduce regularization terms and propose a method, which given an OOD detector for a DNN classifier, learns a set of concepts that have good detection completeness and concept separability (§ 3.3);
- The empirical results with several popular OOD-detectors confirm our insight that concepts with high values for the proposed metrics offer a much clearer distinction in explaining ID- and OOD-detected inputs compared to those with low values (§ 4). We also show how to identify prominent concepts that contribute to an OOD detector’s decisions via a modified Shapley value score that is based on our detection completeness metric (§ 4).

## 2 Problem Setup and Background

**Notations.** Let  $\mathcal{X} \subseteq \mathbb{R}^{a_0 \times b_0 \times d_0}$  denote the space of inputs<sup>1</sup>  $\mathbf{x}$ , where  $d_0$  is the number of channels and  $a_0$  and  $b_0$  are the image size along any channel. Let  $\mathcal{Y} := \{1, \dots, L\}$  denote the space of output class labels  $y$ . Let  $\Delta_L$  denote the set of all probabilities over  $\mathcal{Y}$  (*i.e.*, the simplex in  $L$ -dimensions). We assume that natural inputs to the DNN classifier are sampled from an unknown probability distribution  $P_{\text{in}}$  over the space  $\mathcal{X} \times \mathcal{Y}$ . The compact notation  $[n]$  denotes  $\{1, \dots, n\}$  for a positive integer  $n$ . Boldface symbols are used to denote both vectors and tensors.  $\langle \mathbf{x}, \mathbf{x}' \rangle$  denotes the inner-product between a pair of vectors or image tensors. The indicator function  $\mathbb{1}[c]$  takes value 1 (0) when the condition  $c$  is true (false)

**OOD Detector.** The goal of an OOD detector is to determine if an input to the classifier is ID, *i.e.*,  $(\mathbf{x}, y) \sim P_{\text{in}}$ ; otherwise the input is considered to be OOD. Given a trained classifier  $\mathbf{f}$ , the decision function of an OOD detector can be generally defined as [7],

$$\mathcal{D}_\gamma(\mathbf{x}, \mathbf{f}) = \begin{cases} 1, & \text{if } S(\mathbf{x}, \mathbf{f}) \geq \gamma \\ 0, & \text{otherwise} \end{cases} \quad (1)$$

where  $S(\mathbf{x}, \mathbf{f}) \in \mathbb{R}$  is the score function of the detector for an input  $\mathbf{x} \in \mathcal{X}$  and  $\gamma$  is the threshold. We follow the convention that larger scores correspond to ID inputs, and the detector outputs of 1 and 0 correspond to ID and OOD respectively. Common choices for  $S(\mathbf{x}, \mathbf{f})$  include the softmax confidence score (*i.e.*, the maximum predicted probability) [16], the Energy score computed from logits at the penultimate layer [7], the negative maximum of the unnormalized logits [17], and other combined statistics from the intermediate feature representations [18, 19]. In this work, we assume the availability a pre-trained DNN classifier and a paired OOD detector that is trained to detect inputs to the classifier.

### 2.1 Projection into Concept Space

Consider a pre-trained DNN classifier  $\mathbf{f} : \mathcal{X} \mapsto \Delta_L$  that maps an input  $\mathbf{x}$  to its corresponding predicted class probabilities. Without loss of generality, we can partition the DNN at a convolutional layer  $\ell$  into two parts, *i.e.*,  $\mathbf{f} = \mathbf{h} \circ \phi$  where:

<sup>1</sup>We focus on images, but the ideas extend to other domains.

1)  $\phi : \mathcal{X} \mapsto \mathcal{Z} := \mathbb{R}^{a_\ell b_\ell \times d_\ell}$  (see footnote<sup>2</sup>) is the first half of  $\mathbf{f}$  that maps an input  $\mathbf{x}$  to the intermediate feature representation  $\phi(\mathbf{x})$ , and 2)  $\mathbf{h} : \mathcal{Z} \mapsto \Delta_L$  is the second half of  $\mathbf{f}$  that maps  $\phi(\mathbf{x})$  to the predicted class probability vector  $\mathbf{h}(\phi(\mathbf{x}))$ . We denote the predicted probability of a class  $y$  by  $f_y(\mathbf{x}) = h_y(\phi(\mathbf{x}))$ , and the prediction of the classifier by  $\hat{y}(\mathbf{x}) = \operatorname{argmax}_y f_y(\mathbf{x})$ .

We explore the setting where high-level concepts lie in a subspace of a feature-representation space  $\mathcal{Z}$  of the classifier. Consider a projection matrix  $\mathbf{C} = [\mathbf{c}_1, \dots, \mathbf{c}_m] \in \mathbb{R}^{d_\ell \times m}$  (with  $m \ll d_\ell$ ) that maps from the space  $\mathcal{Z}$  into a reduced-dimension concept space.  $\mathbf{C}$  consists of  $m$  unit (column) vectors  $\mathbf{c}_i$ , which is referred to as a *concept vector* representing the  $i$ -th concept (e.g., "stripe", "oval face", etc.), and  $m$  is the number of concepts. We define the linear projection of a high-dimensional layer representation  $\phi(\mathbf{x}) \in \mathbb{R}^{a_\ell b_\ell \times d_\ell}$  into the concept space by  $\mathbf{v}_C(\mathbf{x}) := \phi(\mathbf{x}) \mathbf{C} \in \mathbb{R}^{a_\ell b_\ell \times m}$ . We also define the mapping from the projected concept space back to the feature space by  $\mathbf{g} : \mathbb{R}^{a_\ell b_\ell \times m} \mapsto \mathbb{R}^{a_\ell b_\ell \times d_\ell}$ . We define this reconstruction of the feature representation at layer  $\ell$  from the concept space by  $\hat{\phi}_{g,C}(\mathbf{x}) := \mathbf{g}(\mathbf{v}_C(\mathbf{x}))$ .

## 2.2 Canonical World and Concept World

As shown in Fig. 2, we consider a "two-world" view of the classifier and OOD detector consisting of a *canonical world* and concept world, defined as follows:

**Canonical World.** In this world, both the classifier and detector use the original layer representation  $\phi(\mathbf{x})$  for their predictions, i.e., the prediction of the classifier is  $\mathbf{f}(\mathbf{x}) = \mathbf{h}(\phi(\mathbf{x}))$ , and the decision function of the detector is  $\mathcal{D}_\gamma(\mathbf{x}, \mathbf{h} \circ \phi)$  with a score function  $S(\mathbf{x}, \mathbf{h} \circ \phi)$ .

**Concept World.** Both the class prediction and OOD detection are based on the reconstructed feature representation  $\hat{\phi}_{g,C}(\mathbf{x})$ . We define the corresponding classifier, detector, and score function in the concept world as follows:

$$\begin{aligned} \mathbf{f}^{\text{con}}(\mathbf{x}) &:= \mathbf{h}(\hat{\phi}_{g,C}(\mathbf{x})) = \mathbf{h}(\mathbf{g}(\mathbf{v}_C(\mathbf{x}))) \\ \mathcal{D}_\gamma^{\text{con}}(\mathbf{x}, \mathbf{f}) &:= \mathcal{D}_\gamma(\mathbf{x}, \mathbf{h} \circ \hat{\phi}_{g,C}) = \mathcal{D}_\gamma(\mathbf{x}, \mathbf{h} \circ \mathbf{g} \circ \mathbf{v}_C) \\ S^{\text{con}}(\mathbf{x}, \mathbf{f}) &:= S(\mathbf{x}, \mathbf{h} \circ \hat{\phi}_{g,C}) = S(\mathbf{x}, \mathbf{h} \circ \mathbf{g} \circ \mathbf{v}_C). \end{aligned} \quad (2)$$

Note that we use the following observation in constructing the concept world: *Both the classifier and the OOD detector can be modified to make predictions based on the reconstructed feature representation (i.e., using  $\hat{\phi}_{g,C}(\mathbf{x})$ ) instead of  $\phi(\mathbf{x})$ .* We elaborate further on this two-world view and introduce two desirable properties: (1) detection completeness and (2) concept separability.

**Detection Completeness.** Given a fixed algorithmic approach for learning the classifier and OOD detector, and with fixed internal parameters of  $\mathbf{f}$ , we would ideally like the classifier prediction and the detection score to be indistinguishable between the two worlds. In other words, for the concepts to *sufficiently* explain the OOD detector, we require that  $\mathcal{D}_\gamma^{\text{con}}(\mathbf{x}, \mathbf{f})$  closely mimic  $\mathcal{D}_\gamma(\mathbf{x}, \mathbf{f})$ . Likewise, we require  $\mathbf{f}^{\text{con}}(\mathbf{x})$  to closely mimic  $\mathbf{f}(\mathbf{x})$  since the detection mechanism of  $\mathcal{D}_\gamma$  is closely paired to the classifier. We refer to this property as the *completeness of a set of concepts with respect to the OOD detector and its paired classifier*. As discussed in Section 3.1, this extends the notion of classification completeness introduced by Yeh *et al.* [15].

**Concept separability.** To improve the interpretability of the resulting explanations for the detector, we require another desirable property on the learned concepts: data detected as ID by  $\mathcal{D}_\gamma$  (henceforth referred to as *detected-ID* data) and data detected as OOD by  $\mathcal{D}_\gamma$  (henceforth referred to as *detected-OOD* data) should be well-separated in the concept-score space. Consider the example in Fig. 1, which shows the concept scores of two input images corresponding to four concepts: "stripe", "oval face", "sky", and "greenery". While both the inputs are predicted into the "Zebra" class by the classifier, the detector predicts one as ID and the other as OOD. The two inputs show clear distinctive patterns for the concepts "stripe" and "oval face", but they have a similar concept-score pattern with respect to the other two concepts "sky" and "greenery". Since our goal is to also guide an analyst to understand which concepts distinguish the detected-ID data from the detected-OOD data, we would like to learn a set of concepts that have a well-separated pattern for pairs from these two groups of inputs, even when classification labels (e.g., zebra) are identical.

## 3 Proposed Approach

Given a trained DNN classifier  $\mathbf{f}$  and a paired OOD detector  $\mathcal{D}_\gamma$ , our goal is to learn a set of concepts that has the desirable properties of detection completeness and concept separability for providing explanations for the detector's

<sup>2</sup>We flatten the first two dimensions of the feature representation, thus changing an  $a_\ell \times b_\ell \times d_\ell$  tensor to an  $a_\ell b_\ell \times d_\ell$  matrix, where  $a_\ell$  and  $b_\ell$  are the filter size and  $d_\ell$  is the number of channels.

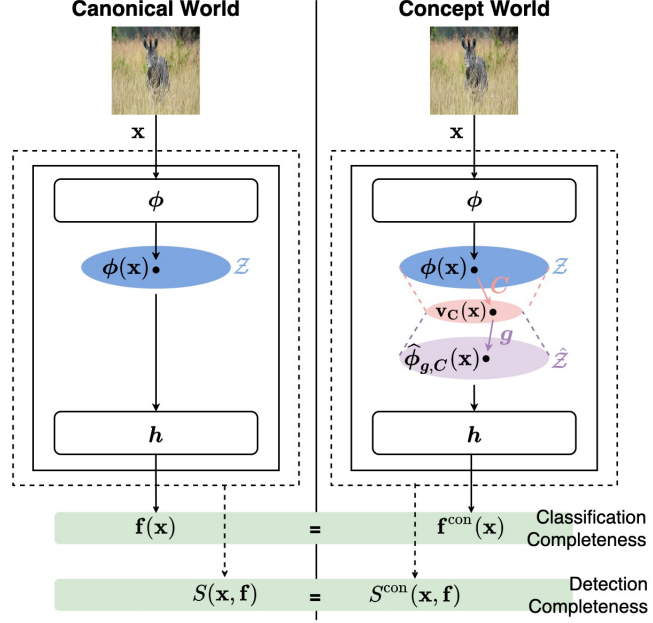


Figure 2: Our two-world view for classifier and detector.

predictions. We first propose new metrics for quantifying the set of learned concepts, followed by a general framework for learning the concepts.

**ID and OOD Datasets.** We assume the availability of a labeled ID training dataset  $D_{\text{in}}^{\text{tr}} = \{(\mathbf{x}_i, y_i), i = 1, \dots, N_{\text{in}}^{\text{tr}}\}$  from the distribution  $P_{\text{in}}$ . We also assume the availability of an unlabeled training dataset  $D_{\text{out}}^{\text{tr}} = \{\tilde{\mathbf{x}}_i, i = 1, \dots, N_{\text{out}}^{\text{tr}}\}$  from a different distribution, referred to as the *auxiliary OOD dataset*. Similarly, we define the ID validation and test datasets (sampled from  $P_{\text{in}}$ ) as  $D_{\text{in}}^{\text{val}}$  and  $D_{\text{in}}^{\text{te}}$ , and the OOD validation and test datasets as  $D_{\text{out}}^{\text{val}}$  and  $D_{\text{out}}^{\text{te}}$ . We note that the auxiliary OOD dataset  $D_{\text{out}}^{\text{tr}}$  and validation OOD dataset  $D_{\text{in}}^{\text{val}}$  are sampled from the same auxiliary distribution (e.g., the MS-COCO dataset). However, the test OOD dataset can be from an entirely different distribution (e.g., the SUN dataset). All the OOD datasets are unlabeled since their label space can be different from  $\mathcal{Y}$ .

**Concept Scores.** We refer the reader to Section 2.1, which introduced a projection matrix  $\mathbf{C} \in \mathbb{R}^{d_{\ell} \times m}$  that maps  $\phi(\mathbf{x})$  to  $\mathbf{v}_C(\mathbf{x})$ , and consists of  $m$  unit concept vectors  $\mathbf{C} := [\mathbf{c}_1 \dots \mathbf{c}_m]$ . The inner product between the feature representation and a concept vector is referred to as the *concept score*, and it quantifies how close an input is to the given concept [20, 12]. Specifically, the concept score corresponding to concept  $i$  is defined as  $\mathbf{v}_{\mathbf{c}_i}(\mathbf{x}) := \langle \phi(\mathbf{x}), \mathbf{c}_i \rangle = \phi(\mathbf{x}) \mathbf{c}_i \in \mathbb{R}^{a_{\ell} b_{\ell}}$ . The matrix of concept scores from all the concepts is simply the concatenation of the individual concept scores, i.e.,  $\mathbf{v}_C(\mathbf{x}) = \phi(\mathbf{x}) \mathbf{C} = [\mathbf{v}_{\mathbf{c}_1}(\mathbf{x}) \dots \mathbf{v}_{\mathbf{c}_m}(\mathbf{x})] \in \mathbb{R}^{a_{\ell} b_{\ell} \times m}$ .

We also define a dimension-reduced version of the concept scores that takes the maximum of the inner-product over each  $a_{\ell} \times b_{\ell}$  patch as follows:  $\tilde{\mathbf{v}}_C(\mathbf{x})^T = [\tilde{v}_{\mathbf{c}_1}(\mathbf{x}), \dots, \tilde{v}_{\mathbf{c}_m}(\mathbf{x})] \in \mathbb{R}^m$ , where  $\tilde{v}_{\mathbf{c}_i}(\mathbf{x}) = \max_{p,q} |\langle \phi^{p,q}(\mathbf{x}), \mathbf{c}_i \rangle| \in \mathbb{R}$ . Here  $\phi^{p,q}(\mathbf{x})$  is the feature representation corresponding to the  $(p, q)$ -th patch of input  $\mathbf{x}$  (i.e., receptive field). This reduction operation is done to capture the most important correlations from each patch, and the  $m$ -dimensional concept score will be used to define our concept separability metric.

### 3.1 Metrics for Detection Completeness

To address the question of whether a set of learned concepts are sufficient to capture the behavior of the classifier and OOD detector, we next define completeness scores with respect to the classification task and the detection task.

**Definition 1.** Given a trained DNN classifier  $\mathbf{f} = \mathbf{h} \circ \phi$  and a set of concept vectors  $\mathbf{C}$ , the *classification completeness* with respect to  $P_{\text{in}}(\mathbf{x}, y)$  is defined as [15]:

$$\eta_{\mathbf{f}}(\mathbf{C}) := \frac{\sup_{\mathbf{g}} \mathbb{E}_{(\mathbf{x}, y) \sim P_{\text{in}}} \mathbb{1}[y = \text{argmax}_{y'} h_{y'}(\hat{\phi}_{\mathbf{g}, \mathbf{C}}(\mathbf{x}))] - a_r}{\mathbb{E}_{(\mathbf{x}, y) \sim P_{\text{in}}} \mathbb{1}[y = \text{argmax}_{y'} h_{y'}(\phi(\mathbf{x}))] - a_r}$$

where  $a_r = 1/L$  is the accuracy of a random predictor.

The denominator of  $\eta_{\mathbf{f}}(\mathbf{C})$  is the accuracy of the original classifier  $\mathbf{f}$ , while the numerator is the maximum accuracy that can be achieved in the concept world using the feature representation reconstructed from the concept scores. In practice, the expectation is estimated using a held-out test dataset  $D_{\text{in}}^{\text{te}}$  from the ID distribution.

**Definition 2.** Given a trained DNN classifier  $\mathbf{f} = \mathbf{h} \circ \phi$ , a trained OOD detector with score function  $S(\mathbf{x}, \mathbf{f})$ , and a set of concept vectors  $\mathbf{C}$ , we introduce a *detection completeness score* with respect to ID distribution  $P_{\text{in}}(\mathbf{x}, y)$  and OOD distribution  $P_{\text{out}}(\mathbf{x})$ , defined as follows:

$$\eta_{\mathbf{f}, S}(\mathbf{C}) := \frac{\sup_{\mathbf{g}} \text{AUC}(\mathbf{h} \circ \hat{\phi}_{\mathbf{g}, \mathbf{C}}) - b_r}{\text{AUC}(\mathbf{h} \circ \phi) - b_r}, \quad (3)$$

where  $\text{AUC}(\mathbf{f})$  is the area under the ROC curve of an OOD detector based on  $\mathbf{f}$ , defined as

$$\text{AUC}(\mathbf{f}) := \mathbb{E}_{(\mathbf{x}, y) \sim P_{\text{in}}} \mathbb{E}_{\mathbf{x}' \sim P_{\text{out}}} \mathbb{1}[S(\mathbf{x}, \mathbf{f}) > S(\mathbf{x}', \mathbf{f})], \quad (4)$$

and  $b_r = 0.5$  is the AUROC of a random detector.

The numerator term is the maximum achievable AUROC in the concept world via reconstructed features from concept scores. In practice,  $\text{AUC}(\mathbf{f})$  is estimated using test datasets from the ID and OOD, *i.e.*,  $D_{\text{in}}^{\text{te}}$  and  $D_{\text{out}}^{\text{te}}$ .

Both the classification completeness and detection completeness scores are designed to be in the range  $[0, 1]$ . However, this is not strictly guaranteed since the classifier or OOD detector in the concept world may empirically have a better (corresponding) metric on a given ID/OOD dataset. A completeness score close to 1 indicates that the set of concepts  $\mathbf{C}$  are close to complete in characterizing the behavior of the classifier and/or the OOD detector.

### 3.2 Concept Separability Score

To ensure better interpretability of the concept-based explanations for OOD detection, we pose the question: *do the set of concepts show clear distinctions in their scores between detected-ID data and detected-OOD data?* Formally, we would like the set of concept-score vectors from the detected-ID class  $V_{\text{in}}(\mathbf{C}) := \{\tilde{\mathbf{v}}_{\mathbf{C}}(\mathbf{x}), \mathbf{x} \in D_{\text{in}}^{\text{tr}} \cup D_{\text{out}}^{\text{tr}} : \mathcal{D}_{\gamma}(\mathbf{x}, \mathbf{f}) = 1\}$ , and the set of concept-score vectors from the detected-OOD class  $V_{\text{out}}(\mathbf{C}) := \{\tilde{\mathbf{v}}_{\mathbf{C}}(\mathbf{x}), \mathbf{x} \in D_{\text{in}}^{\text{tr}} \cup D_{\text{out}}^{\text{tr}} : \mathcal{D}_{\gamma}(\mathbf{x}, \mathbf{f}) = 0\}$  to be well separated. Let  $J_{\text{sep}}(V_{\text{in}}(\mathbf{C}), V_{\text{out}}(\mathbf{C})) \in \mathbb{R}$  define a general *measure of separability* between the two data subsets, such that a larger value corresponds to higher separability. We discuss specific choices for  $J_{\text{sep}}$  for which it is possible to tractably optimize the concept separability as part of the learning objective.

**Global Concept Separability.** Class separability metrics have been well studied in the pattern recognition literature, particularly for the two-class case [21]<sup>3</sup>. Motivated by Fisher's linear discriminant analysis (LDA), we explore the use of class-separability measures based on the within-class and between-class scatter matrices [22]. The goal of LDA is to find a projection vector (direction) such that data from the two classes are maximally separated and form compact clusters upon projection. Rather than finding an optimal projection direction, we are more interested in ensuring that the concept-score vectors from the detected-ID and detected-OOD data have high separability. Consider the within-class and between-class scatter matrices based on  $V_{\text{in}}(\mathbf{C})$  and  $V_{\text{out}}(\mathbf{C})$ , given by

$$\mathbf{S}_w = \sum_{\mathbf{v} \in V_{\text{in}}(\mathbf{C})} (\mathbf{v} - \boldsymbol{\mu}_{\text{in}})(\mathbf{v} - \boldsymbol{\mu}_{\text{in}})^T + \sum_{\mathbf{v} \in V_{\text{out}}(\mathbf{C})} (\mathbf{v} - \boldsymbol{\mu}_{\text{out}})(\mathbf{v} - \boldsymbol{\mu}_{\text{out}})^T, \quad (5)$$

$$\mathbf{S}_b = (\boldsymbol{\mu}_{\text{out}} - \boldsymbol{\mu}_{\text{in}})(\boldsymbol{\mu}_{\text{out}} - \boldsymbol{\mu}_{\text{in}})^T, \quad (6)$$

where  $\boldsymbol{\mu}_{\text{in}}$  and  $\boldsymbol{\mu}_{\text{out}}$  are the mean concept-score vectors from  $V_{\text{in}}(\mathbf{C})$  and  $V_{\text{out}}(\mathbf{C})$  respectively. We define the following separability metric between based on the generalized eigenvalue equation solved by Fisher's LDA [21]:

$$J_{\text{sep}}(\mathbf{C}) := J_{\text{sep}}(V_{\text{in}}(\mathbf{C}), V_{\text{out}}(\mathbf{C})) = \text{tr}[\mathbf{S}_w^{-1} \mathbf{S}_b]. \quad (7)$$

Maximizing the above metric is equivalent to maximizing the sum of eigenvalues of the matrix  $\mathbf{S}_w^{-1} \mathbf{S}_b$ , which in-turn ensures a large between-class separability and a small within-class separability for the detected-ID and detected-OOD concept scores. We refer to this as a *global concept separability* metric because it does not analyze the separability on a per-class level. The separability metric is closely related to the Bhattacharya distance, which is an upper bound on the Bayes error rate (see Appendix A.1).

**Per-Class Variations.** We also propose per-class measures for detection completeness and concept separability. One can simply compute Eqn. (3) and Eqn. (7) using the subset of ID and OOD data whose predictions are class  $y \in [L]$ . We refer to these per-class variations as *per-class detection completeness* (denoted by  $\eta_{\mathbf{f}, S}^y(\mathbf{C})$ ) and *per-class concept separability* (denoted by  $J_{\text{sep}}^y(\mathbf{C})$ ). For the formal definitions, please refer to Appendix A.2 and A.3.

<sup>3</sup>The two classes correspond to detected-ID and detected-OOD.

### 3.3 Proposed Concept Learning – Key Ideas

**Prior Approaches to Concept Learning.** Prior work on concept learning provides explanations that are more aligned with human reasoning and has been applied to DNN classifiers. Given a DNN classifier, [20], [12] and [15] are post-hoc concept-discovery methods to find concept vectors in the space supported by the intermediate feature representations of ID training data. Unlike [20] and [12], that do not support imposing required conditions into the concept discovery, [15] devised a learning-based approach where classification completeness and the saliency of concepts are optimized via a regularized objective given by

$$\operatorname{argmax}_{\mathbf{C}, \mathbf{g}} \mathbb{E}_{(\mathbf{x}, y) \sim P_{\text{in}}} [\log h_y(\mathbf{g}(\mathbf{v}_{\mathbf{C}}(\mathbf{x})))] + \lambda_{\text{expl}} R_{\text{expl}}(\mathbf{C}). \quad (8)$$

Here  $\mathbf{C}$  and  $\mathbf{g}$  (parameterized by a neural network) are jointly optimized, and  $R_{\text{expl}}(\mathbf{C})$  is a regularization term used to ensure that the learned concept vectors have high spatial coherency and low redundancy among themselves. Specifically, the regularization term is given by [15]

$$R_{\text{expl}}(\mathbf{C}) = \frac{1}{mK} \sum_{i=1}^m \sum_{\mathbf{x}' \in T_{\mathbf{c}_i}} \langle \phi(\mathbf{x}'), \mathbf{c}_i \rangle - \frac{1}{m(m-1)} \sum_{i=1}^m \sum_{j=i+1}^m \langle \mathbf{c}_i, \mathbf{c}_j \rangle \quad (9)$$

where  $T_{\mathbf{c}_i}$  is the set of  $K$ -nearest neighbor patches of the concept vector  $\mathbf{c}_i$  from the ID training set  $D_{\text{in}}^{\text{tr}}$ .

**Limitations of Prior Work for OOD detectors.** While the objective (8) of [15] can learn a set of sufficient concepts that have a high classification completeness score, we found that it does not necessarily replicate the per-instance prediction behavior of the classifier in the concept world. Specifically, there can be discrepancies in the reconstructed feature representation, whose effect propagates through to the output of the classifier. For instance, the empirical distribution of the prediction logits (pre-softmax layer) for both ID and OOD data based on the reconstructed feature representations could be very different from that based on the original feature representations. Since many widely-used OOD detectors rely on the feature representations and/or the classifier’s predictions, this discrepancy in the existing concept learning approaches makes it hard to closely replicate the OOD detector in the concept world. Moreover, the scope of [15] is confined to concept learning for explaining the classifier’s predictions based on ID data, and there is no guarantee that their learned concepts would be useful for explaining an OOD detector. In fact, the distribution of concept scores from ID and OOD data could be quite different (see Fig. 3). To address these gaps, we propose a general method for concept learning that complements prior works by imposing additional instance-level constraints on the concepts, and by taking into consideration the OOD detector and OOD data.

**Concept Learning Objective.** Our concept learning objective aims to find a set of concepts  $\mathbf{C}$  and a mapping  $\mathbf{g}$  that have the following properties: 1) high detection completeness w.r.t the OOD detector; 2) high classification completeness w.r.t the DNN classifier; and 3) high separability in the concept-score space between detected-ID data and detected-OOD data.

Inspired by recent works on transferring feature information from a teacher model to a student model [23, 24, 25], we propose to introduce additional regularization terms into the concept learning objective. In order to encourage accurate reconstruction of  $\hat{\mathcal{Z}}$  based on the concept scores, we introduce a regularization term that is the squared- $\ell_2$  distance between the original and reconstructed representations:

$$J_{\text{norm}}(\mathbf{C}, \mathbf{g}) = \mathbb{E}_{\mathbf{x} \sim P_{\text{in}}} \|\phi(\mathbf{x}) - \hat{\phi}_{\mathbf{g}, \mathbf{C}}(\mathbf{x})\|^2. \quad (10)$$

In order to encourage the scores of the OOD detector in the concept world and canonical world to be close to each other on a per-sample level, we introduce the following mean-squared-error (MSE) based regularization term:

$$J_{\text{mse}}(\mathbf{C}, \mathbf{g}) = \mathbb{E}_{\mathbf{x} \sim P_{\text{in}}} (S(\mathbf{x}, \mathbf{h} \circ \hat{\phi}_{\mathbf{g}, \mathbf{C}}) - S(\mathbf{x}, \mathbf{f}))^2 + \mathbb{E}_{\mathbf{x} \sim P_{\text{out}}} (S(\mathbf{x}, \mathbf{h} \circ \hat{\phi}_{\mathbf{g}, \mathbf{C}}) - S(\mathbf{x}, \mathbf{f}))^2. \quad (11)$$

We include MSE terms from both the ID and OOD data because we want to ensure that the ROC curve corresponding to both the score functions are close to each other (which requires OOD data). Finally, in order to enhance the interpretability of our concept-based explanations, we introduce a regularization term to maximize the separability metric between the detected-ID and detected-OOD data in the concept-score space. With all regularization terms included, our final concept learning objective is given by

$$\begin{aligned} & \operatorname{argmax}_{\mathbf{C}, \mathbf{g}} \mathbb{E}_{(\mathbf{x}, y) \sim P_{\text{in}}} [\log h_y(\mathbf{g}(\mathbf{v}_{\mathbf{C}}(\mathbf{x})))] + \lambda_{\text{expl}} R_{\text{expl}}(\mathbf{C}) \\ & - \lambda_{\text{mse}} J_{\text{mse}}(\mathbf{C}, \mathbf{g}) - \lambda_{\text{norm}} J_{\text{norm}}(\mathbf{C}, \mathbf{g}) + \lambda_{\text{sep}} J_{\text{sep}}(\mathbf{C}). \end{aligned} \quad (12)$$

Note that the sign on the  $\ell_2$  norm-based regularization and the MSE regularization terms is negative since we aim to minimize them. We use stochastic gradient descent-based optimization with adaptive learning rate (specifically

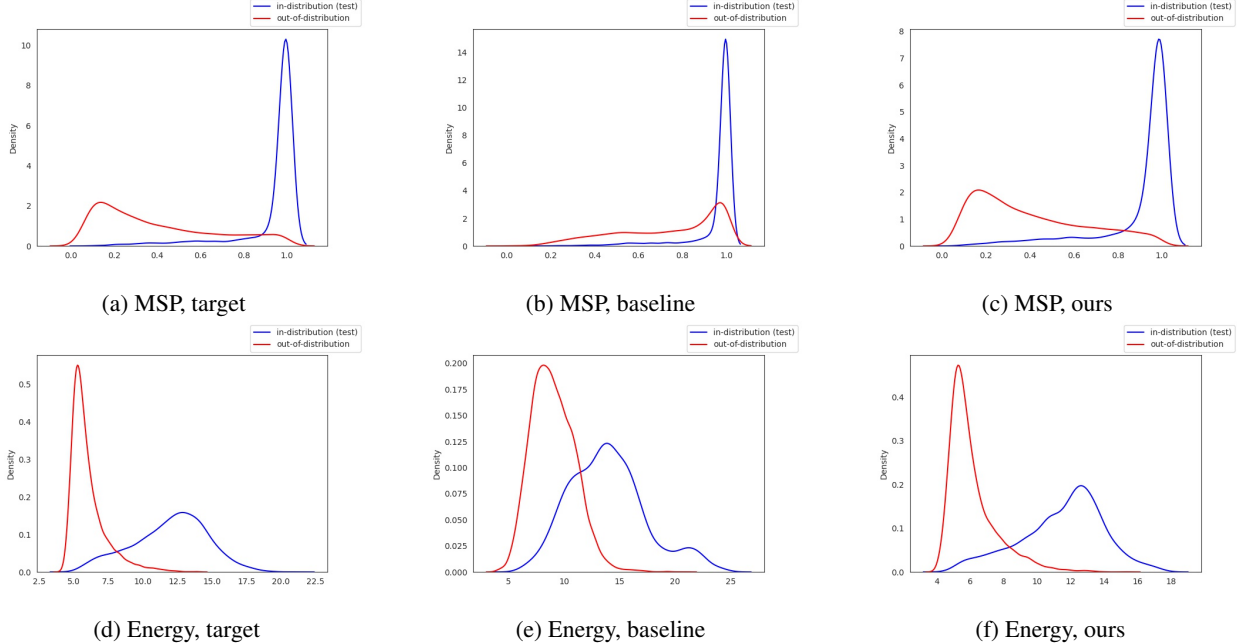


Figure 3: Estimated density of the score  $S(\mathbf{x}, \mathbf{f})$  on the AwA test data (ID: blue) and the SUN dataset (OOD: red). The DNN classifier is Inception-V3 and the OOD detector is either MSP or Energy. **Left:** Target distribution of  $S(\mathbf{x}, \mathbf{f})$  in the canonical world. **Mid:** Distribution of  $S^{\text{con}}(\mathbf{x}, \mathbf{f})$  in the concept world, using concepts learned by [15] (*i.e.*,  $\lambda_{\text{mse}} = \lambda_{\text{norm}} = \lambda_{\text{sep}} = 0$ ). **Right:** Distribution of  $S^{\text{con}}(\mathbf{x}, \mathbf{f})$  in the concept world, using concepts learned by our method. For MSP we set  $\lambda_{\text{mse}} = 10$ ,  $\lambda_{\text{norm}} = 0.1$ ,  $\lambda_{\text{sep}} = 0$ , and for Energy we set  $\lambda_{\text{mse}} = 1$ ,  $\lambda_{\text{norm}} = 0.1$ ,  $\lambda_{\text{sep}} = 0$ .

Adam [26]) to solve the learning objective. The expectations involved in each of the terms in the objective are calculated using sample estimates from the training ID and OOD datasets. Specifically,  $D_{\text{in}}^{\text{tr}}$  is used to compute the expectation over  $P_{\text{in}}$ , and  $D_{\text{out}}^{\text{tr}}$  is used to compute the expectation over  $P_{\text{out}}$ . We summarize our complete concept learning algorithm in Algorithm 1 (see Appendix A.4).

## 4 Experiments

In this section, we carry out experiments to evaluate the proposed method and address the following questions:

- Q1.** Does our concept learning objective effectively encourage concepts to have the desired properties of detection completeness and concept separability?
- Q2.** Are the proposed evaluation metrics effective at providing better interpretability for the resulting concept-based explanations?
- Q3.** Given concepts learned by our approach, what insights can we provide for well-known OOD detectors?

To answer these questions, we apply our framework to interpret four popular OOD detectors from the literature: MSP [16], ODIN [27], Energy [7] and Mahalanobis [18] (henceforth abbreviated to Mahal). The OOD detectors are paired with the widely-used Inception-V3 model [28] (following the setup in prior works [15, 12, 20]), trained on the Animals-with-Attributes (AwA) dataset [29], which yields a test accuracy of 0.921.

Our main findings are summarized as follows:

- A1.** The regularization terms in our concept learning objective effectively improve detection completeness and concept separability, without sacrificing the classification completeness. For instance, given the ODIN detector and the SUN dataset [30] as OOD data, including our proposed regularization terms improves the detection completeness of concepts from 0.869 to 0.969, and the relative concept separability is increased by 0.356, compared to when concepts are learned without the regularization terms (see Table 1).
- A2.** Concepts with a high completeness score enable to mimic the original behavior of the OOD detector more precisely, hence leading to more accurate explanations based on the concepts (see Fig. 3). Also, concepts with a higher concept separability score lead to more visually-distinctive interpretations between ID and OOD data

OOD detector	Hyperparameters	$\eta_f(\mathbf{C})$	OOD data							
			Places		SUN		Textures		iNaturalist	
			$\eta_{f,S}(\mathbf{C})$	$J_{sep}(\mathbf{C}, \mathbf{C}')$						
MSP	$\lambda_{mse} = 0, \lambda_{norm} = 0, \lambda_{sep} = 0$	0.990	0.849	0.0	0.848	0.0	0.824	0.0	0.958	0.0
	$\lambda_{mse} = 10, \lambda_{norm} = 0.1, \lambda_{sep} = 0$	<b>0.994</b>	0.947	0.216	0.946	0.118	0.922	<b>0.406</b>	<b>0.970</b>	0.175
	$\lambda_{mse} = 0, \lambda_{norm} = 0, \lambda_{sep} = 50$	0.980	0.815	<b>0.412</b>	0.816	<b>0.303</b>	0.773	0.376	0.863	0.267
	$\lambda_{mse} = 10, \lambda_{norm} = 0.1, \lambda_{sep} = 50$	0.985	<b>0.959</b>	0.327	<b>0.961</b>	0.266	<b>0.938</b>	0.344	0.946	<b>0.286</b>
ODIN	$\lambda_{mse} = 0, \lambda_{norm} = 0, \lambda_{sep} = 0$	0.990	0.869	0.0	0.869	0.0	0.850	0.0	0.981	0.0
	$\lambda_{mse} = 10^8, \lambda_{norm} = 0.1, \lambda_{sep} = 0$	<b>0.994</b>	0.951	0.161	0.959	0.215	0.936	0.411	0.936	0.151
	$\lambda_{mse} = 0, \lambda_{norm} = 0, \lambda_{sep} = 50$	0.987	0.899	<b>0.373</b>	0.911	0.342	0.790	<b>0.414</b>	0.970	<b>0.337</b>
	$\lambda_{mse} = 10^8, \lambda_{norm} = 0.1, \lambda_{sep} = 50$	0.991	<b>0.973</b>	0.355	<b>0.969</b>	<b>0.356</b>	<b>0.945</b>	0.405	<b>0.982</b>	0.308
Energy	$\lambda_{mse} = 0, \lambda_{norm} = 0, \lambda_{sep} = 0$	0.990	0.845	0.0	0.847	0.0	0.832	0.0	0.973	0.0
	$\lambda_{mse} = 1, \lambda_{norm} = 0.1, \lambda_{sep} = 0$	<b>0.993</b>	0.965	0.135	0.963	0.127	0.960	0.284	0.949	0.215
	$\lambda_{mse} = 0, \lambda_{norm} = 0, \lambda_{sep} = 50$	0.987	0.779	<b>0.422</b>	0.794	0.371	0.767	<b>0.510</b>	0.911	<b>0.288</b>
	$\lambda_{mse} = 1, \lambda_{norm} = 0.1, \lambda_{sep} = 50$	0.990	<b>0.971</b>	0.365	<b>0.970</b>	<b>0.400</b>	<b>0.964</b>	0.494	<b>0.973</b>	0.280
Mahal	$\lambda_{mse} = 0, \lambda_{norm} = 0, \lambda_{sep} = 0$	0.990	0.860	0.0	0.860	0.0	0.831	0.0	0.972	0.0
	$\lambda_{mse} = 0.1, \lambda_{norm} = 0.1, \lambda_{sep} = 0$	<b>0.994</b>	0.962	0.153	0.963	0.176	0.962	0.351	0.955	0.169
	$\lambda_{mse} = 0, \lambda_{norm} = 0, \lambda_{sep} = 50$	0.985	0.850	<b>0.430</b>	0.883	0.362	0.774	<b>0.429</b>	0.926	<b>0.386</b>
	$\lambda_{mse} = 0.1, \lambda_{norm} = 0.1, \lambda_{sep} = 50$	0.991	<b>0.971</b>	0.370	<b>0.970</b>	<b>0.388</b>	<b>0.970</b>	0.397	<b>0.972</b>	0.351

Table 1: **Results of concept learning with different parameter settings across various OOD detectors and OOD datasets.** Larger values are better for all the metrics. **Bold** numbers indicate the best results (across the rows) for a given OOD detection method and dataset. Note that by definition of  $J_{sep}(\mathbf{C}, \mathbf{C}')$  (Eqn. 13), the relative concept separability of the baseline [15] is always 0, *i.e.*,  $J_{sep}(\mathbf{C}', \mathbf{C}') = 0$ .

compared to concepts with a lower concept separability score, by having more distinguishable concept-score patterns (see Fig. 4).

**A3.** We can rank the importance of each concept towards OOD detection using the Shapley value modified with our per-class detection completeness metric. When the concepts are only targeted at explaining the DNN classifier (as in the baseline [15]), the behavior of the OOD detector is merely described by the common set of concepts that are important for the DNN classifier. On the other hand, when not only the DNN classifier but also the OOD detector is taken into consideration during concept learning (*i.e.*, our method), we obtain a more diverse and expanded set of concepts, and different concepts play a major role in interpreting the classification and detection results (see Fig. 5).

#### 4.1 Setup

**Datasets.** For the ID dataset, we use Animals with Attributes (AwA) [29] with 50 animal classes, and split it into a train set (with 29841 images), validation set (with 3709 images), and test set (with 3772 images). We use the MSCOCO dataset [31] as the auxiliary OOD dataset  $D_{out}^{tr}$  for training and validation. For the OOD test dataset  $D_{out}^{te}$ , we follow a common setting in the literature of large-scale OOD detection [32] and use four different image datasets: Places365 [33], SUN [30], Textures [34], iNaturalist [35]; all resized to the input size  $224 \times 224$ .

**Metrics.** For each set of concepts learned with different OOD detectors and hyperparameters, we report the classification completeness  $\eta_f(\mathbf{C})$ , detection completeness  $\eta_{f,S}(\mathbf{C})$ , and the relative concept separability metric (defined below). In contrast to the completeness scores that are almost always bounded to the range  $[0, 1]$ <sup>4</sup>, it is hard to gauge the possible range of the separability score  $J_{sep}(\mathbf{C})$  (or  $J_{sep}^y(\mathbf{C})$ ) across different settings (datasets, classification models, and OOD detectors), and whether the value represents a significant improvement in separability. Hence, we define the *relative concept separability*, which captures the relative improvement in concept separability between two different sets of concepts, as follows

$$J_{sep}(\mathbf{C}, \mathbf{C}') = \text{Median} \left( \left\{ \frac{J_{sep}^y(\mathbf{C}) - J_{sep}^y(\mathbf{C}')}{J_{sep}^y(\mathbf{C}')} \right\}_{y=1}^L \right). \quad (13)$$

This metric measures the median of the relative increase in the per-class separability using concepts  $\mathbf{C}$ , compared to that of using a different set of concepts  $\mathbf{C}'$ . We choose  $\mathbf{C}'$  to be the set of concepts learned by the baseline [15], which is a special case of our learning objective when  $\lambda_{mse} = \lambda_{norm} = \lambda_{sep} = 0$ . The set of concept  $\mathbf{C}$  are obtained via our concept learning objective, with various combinations of hyperparameter values. For details on the hyperparameter setting, see Appendix A.5.

<sup>4</sup>In general, we observe that the performance of the classifier and OOD detector in the concept world does not exceed that of the canonical world.

## 4.2 Effectiveness of Our Method

In this subsection, we elaborate on the experiments to answer the first question (Q1) on the effectiveness of our concept learning objective. The results are summarized in Table 1 for different OOD detection methods and OOD datasets. We consider the following four settings of the hyperparameters in order to evaluate the effectiveness of the proposed regularization terms in the concept-learning objective: **i**) all the hyperparameters are set to 0 (first row), which corresponds to the baseline method [15]; **ii**) only the regularization terms for reconstruction error  $J_{\text{norm}}(\mathbf{C}, \mathbf{g})$  and mean-squared error  $J_{\text{mse}}(\mathbf{C}, \mathbf{g})$  are included (second row); **iii**) only the regularization term for concept separability  $J_{\text{sep}}(\mathbf{C})$  is included (third row); **iv**) all the regularization terms are included (fourth row).

From Table 1, we observe that the regularization terms  $J_{\text{norm}}(\mathbf{C}, \mathbf{g})$  and  $J_{\text{mse}}(\mathbf{C}, \mathbf{g})$  improve not only the detection completeness by a large margin, but also the classification completeness, compared to the (baseline) case where  $\lambda_{\text{norm}} = \lambda_{\text{mse}} = 0$ . This validates our hypothesis that accurate reconstruction of the feature representation space  $\hat{\mathcal{Z}}$  and the score functions are both crucial for closing the performance gap between the canonical world and concept world of both the classifier and the OOD detector. We observe that the relative concept separability  $J_{\text{sep}}(\mathbf{C}, \mathbf{C}')$  is largest most often for the setting where  $\lambda_{\text{mse}} = \lambda_{\text{norm}} = 0$ , and  $\lambda_{\text{sep}} > 0$  (third row). However, the detection completeness does not improve and in some cases drops compared to the baseline setting, suggesting that there is a tradeoff between maximizing the detection completeness and concept separability.

Finally, our method achieves the best detection completeness in most of the cases for the setting where *all* the regularization terms are included, *i.e.*,  $\lambda_{\text{mse}} > 0$ ,  $\lambda_{\text{norm}} > 0$ , and  $\lambda_{\text{sep}} > 0$ . In this setting, there is a slight decrease the relative concept separability compared to the case where only the regularization term  $J_{\text{sep}}(\mathbf{C})$  is included (third row). In other words, there is a tradeoff wherein we may have to sacrifice the concept separability a little in order to achieve the best possible detection completeness. Further investigation including an ablation study on each regularization term can be found in Appendix A.6. Interestingly, we observe that the concepts targeted for a particular type of OOD detector can also be applied to different types of OOD detectors (*i.e.*, the learned concepts exhibit transferability). Refer to Appendix A.6 for the full discussion on concept transferability.

## 4.3 Interpretability of the Learned Concepts

We provide further insights on the interpretability of the learned concepts in order to address the second question (Q2). Specifically, we demonstrate that the concepts learned by our method enable more *accurate*, and more *visually distinctive* interpretations, compared to the concepts learned by the baseline method ([15]).

**Detection completeness and accurate reconstruction of  $\mathcal{Z}$ .** In Fig. 3, we compare the distribution of the OOD detector scores in the canonical world and concept world using the concepts learned by our method and by [15] (having different detection completeness). The distribution of  $S^{\text{con}}(\mathbf{x}, \mathbf{f})$  calculated based on the concepts learned by [15] (with detection completeness  $\eta_{\mathbf{f}, S}(\mathbf{C}) = 0.85$  for both the MSP and Energy detectors) is significantly different from that of the target distribution of  $S(\mathbf{x}, \mathbf{f})$ . See Fig. 3a vs. Fig. 3b, and Fig. 3d vs. Fig. 3e. This suggests that the concepts learned by [15] can lead to a strong mis-match between the score distributions on both ID data and OOD data.

In contrast,  $S^{\text{con}}(\mathbf{x}, \mathbf{f})$  calculated based on the concepts learned by our method (with  $\eta_{\mathbf{f}, S}(\mathbf{C}) = 0.95$  for the MSP detector, and  $\eta_{\mathbf{f}, S}(\mathbf{C}) = 0.97$  for the Energy detector) approximates the target score distributions more closely on both ID data and OOD data. See Fig. 3a vs. Fig. 3c, and Fig. 3d vs. Fig. 3f. Overall, our experiments find that the proposed regularization terms reduce the performance gap (between the canonical world and concept world) of both the classifier and the OOD detector. This enables more accurate concept-based explanations for an OOD detector.

**Concept separability and distinction in explanations.** We investigate whether the concepts with a higher concept-separability measure lead to a more distinguishable pattern between the concept scores of detected-ID inputs and detected-OOD inputs. Fig. 4 illustrates the concept score patterns of two different sets of concepts having different concept separability scores. We take the average of concept scores  $V_{\text{in}}(\mathbf{C})$  (or  $V_{\text{out}}(\mathbf{C})$ ) among the inputs that are predicted as class  $y$ , and detected as ID (or OOD) by the OOD detector (Energy-based OOD detection is used in this case). When using concepts that correspond to a relatively low per-class concept separability ( $J_{\text{sep}}^y(\mathbf{C}) = 0.059$ ), we fail to observe any noticeable difference in the concept scores of detected-ID and detected-OOD data (see Figs. 4a and 4c). On the other hand, concepts with a higher per-class concept separability ( $J_{\text{sep}}^y(\mathbf{C}) = 0.098$ ) show clear distinguishable patterns between detected-ID and detected-OOD data (see Figs. 4b and 4d). These observations confirm our design motivation for the concept separability metric – that a higher value of the concept separability metric enables better visual distinction between the concept score patterns, suggesting better interpretability for humans.

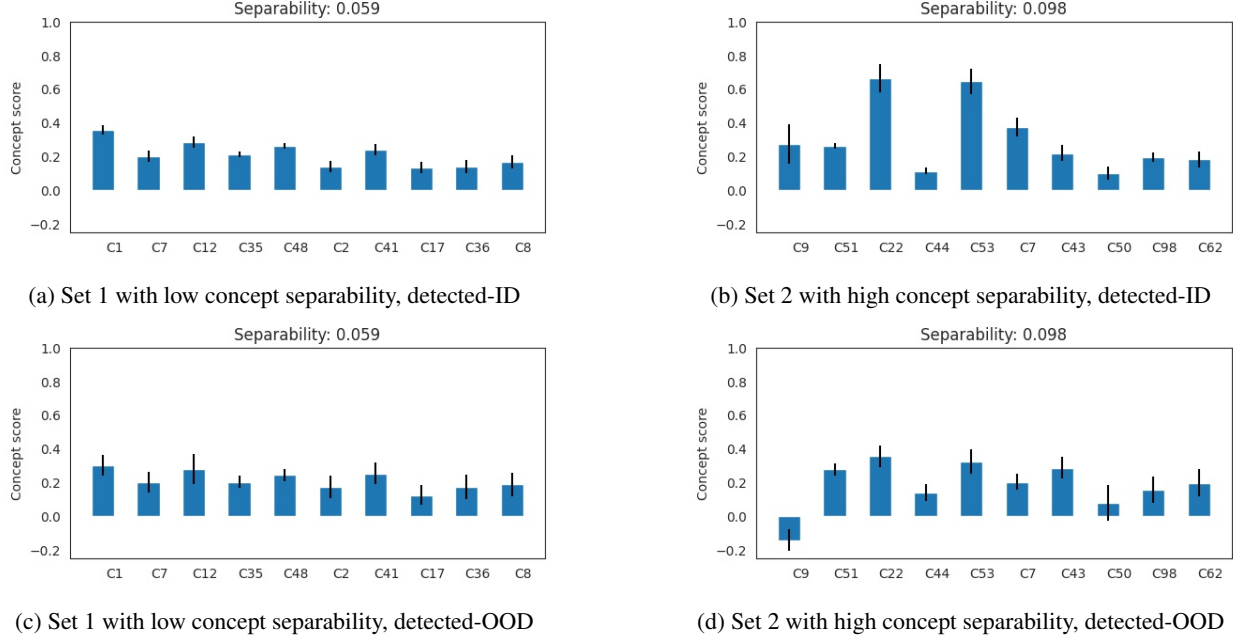


**Figure 4: Our concept separability metric and visual distinction in the concept score patterns.** For the class "Giraffe", we compare the concept score patterns using two different sets of concepts. **Left:** Averaged concept scores using concept set 1 (top-10 important concepts out of the concepts learned with  $\lambda_{mse} = \lambda_{norm} = \lambda_{sep} = 0$ ). **Right:** Averaged concept scores using concept set 2 (top-10 important concepts out of the concepts learned with  $\lambda_{mse} = 1, \lambda_{norm} = 0.1, \lambda_{sep} = 50$ ). Concept importance is measured using the Shapley value of Eqn. (14). Concept separability is measured based on the presented 10 concepts from each set.

#### 4.4 Concept-based Explanations for OOD Detectors

Lastly, we illustrate how the concepts learned by our algorithm can be used to provide explanations for an OOD detector (addressing the last question (Q3)). By quantifying the contribution of each concept toward OOD detection results, we can identify the major concepts that an OOD detector relies on to make decisions.

**Contribution of each concept to detection.** The proposed concept learning algorithm learns concepts for both the classifier and OOD detector considering all the classes. Among all the concepts, we would like to specify the most prominent concepts required for understanding the OOD detector with respect to a particular class. We address the following question: *how much does each concept contribute to the detection results for inputs predicted to a particular class?*. Recent works have adopted the Shapley value from Coalitional Game theory literature [36, 37] for scoring the importance of a feature subset towards the predictions of a model [38, 39, 40]. Extending this idea, we modify the characteristic function of the Shapley value using our per-class detection completeness metric (Eqn. (15) in Appendix A.2). The modified Shapley value of a concept  $\mathbf{c}_i \in \mathbf{C}$  with respect to the predicted class  $j \in [L]$  is defined as

$$\text{SHAP}(\eta_{f,S}^j, \mathbf{c}_i) := \sum_{\mathbf{C}' \subseteq \mathbf{C} \setminus \{\mathbf{c}_i\}} \frac{(m - |\mathbf{C}'| - 1)! |\mathbf{C}'|!}{m!} (\eta_{f,S}^j(\mathbf{C}' \cup \{\mathbf{c}_i\}) - \eta_{f,S}^j(\mathbf{C}')), \quad (14)$$

where  $\mathbf{C}'$  is a subset of  $\mathbf{C}$  excluding concept  $\mathbf{c}_i$ , and  $\eta_{f,S}^j$  is the (per-class) detection completeness with respect to class  $j$ . This Shapley value captures the average marginal contribution (*i.e.*, importance) of concept  $\mathbf{c}_i$  towards explaining the decisions of the OOD detector for inputs that are predicted by the classifier into class  $j$ .

Based on this concept importance metric, we present the top-ranked concepts along with the visualized examples that are nearest to the corresponding concept vector in Fig. 5. For the baseline method [15] (denoted "baseline" in Fig. 5), the learned concepts are solely intended for reconstructing the behavior of the classifier. In this case, we observe from Fig. 5 that interpretation of both the classifier and OOD detector depends on a common set of concepts (*i.e.*, concepts 32, 10, and 47). On the other hand, the concepts learned by our method focus on reconstructing the behavior of both the OOD detector and the classifier. In this case, we observe from Fig. 5 that a distinct set of important concepts are selected for classification and OOD detection. We also observe that our method requires more concepts in order to address the decisions of both the classifier and OOD detector. For instance, the number of concepts obtained by our

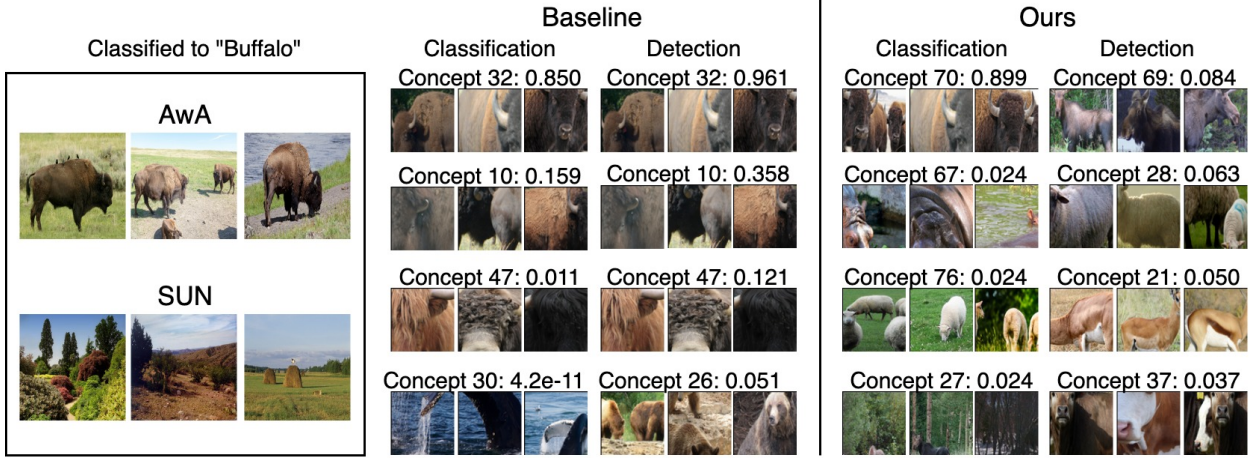


Figure 5: **Most important concepts for the Energy detector with respect to the predicted class “Buffalo”.** We demonstrate randomly sampled images that are predicted by the classifier into this class. We compare the top-4 important concepts to describe the DNN classifier (and Energy detector), ranked by the Shapley value based on classification completeness  $\text{SHAP}(\eta_f^j, \mathbf{c}_i)$  (and detection completeness  $\text{SHAP}(\eta_{f,S}^j, \mathbf{c}_i)$ ). “Baseline” corresponds to the case when the concepts are learned with  $\lambda_{\text{mse}} = \lambda_{\text{norm}} = \lambda_{\text{sep}} = 0$ , whereas “Ours” corresponds to the concepts learned with  $\lambda_{\text{mse}} = 1, \lambda_{\text{norm}} = 0.1, \lambda_{\text{sep}} = 0$ . To visualize what each concept represents, we display the top receptive fields from  $D_{\text{in}}^{\text{te}}$  whose inner-product with the corresponding concept vector is larger than 0.8.

method and the baseline are 78 and 53 (respectively), out of a total 100 concepts<sup>5</sup>. More examples of concepts with high-ranking Shapley scores can be found in Appendix B.1. We further investigate the attribution of such top-ranked concepts via counterfactual analysis in Appendix B.2.

## 5 Related Work

**OOD detection.** Starting with a simple baseline for OOD detection based on the maximum softmax probability (MSP) score [16], recent studies have designed various scoring functions based on the outputs from the final or penultimate layers [27, 41], or a combination of different intermediate layers of DNN model [18]. Our general framework can be applied to these existing OOD detection methods by choosing a suitable intermediate layer for concept-based interpretation<sup>6</sup>. To further improve the OOD uncertainty estimation, several works attempt to finetune the DNN classifier using auxiliary OOD training data [4, 42, 8]. Complementary to these, our work is a post-hoc method that aims to explain an already-trained DNN model and its paired OOD detector. Our concept learning algorithm discovers concepts through optimization based on the feature representations from a DNN layer, without modifying the internals of the DNN or the OOD detector.

**Post-hoc interpretability.** Feature attribution is the most commonly used post-hoc explanation method that attributes the decision to local input features [43, 44, 45, 9], but recent works have demonstrated its vulnerability to *e.g.*, adversarial perturbations [46, 47, 48]. Adebayo *et al.* [11] also conduct experimental analyses and a human subject study to assess the effectiveness of feature attributions under various settings (including on OOD data), and show that feature attributions barely have any visual difference between ID inputs and OOD inputs.

On the other hand, concept-based explanation is another type of interpretation method, which is designed to be better-aligned with human reasoning [49, 50] and intuition [12, 13, 14, 15]. A common implicit assumption in the concept-based explanation literature is *linear interpretability*, *i.e.*, the concepts lie in a linearly-projected subspace of intermediate DNN layer activations; our work is also based on this assumption. While the scope of existing works is confined to explaining DNN classifiers, we extend the use of concept-based interpretability for explaining OOD detectors. Our work is inspired by [15], and we extend their concept-based explanation method for DNN classifiers to OOD detectors. As discussed in section 3.3, the concept learning objective of [15] can be obtained as a special case of our concept learning objective for the hyper-parameter setting  $\lambda_{\text{norm}} = \lambda_{\text{mse}} = \lambda_{\text{sep}} = 0$ .

<sup>5</sup>After removing redundant concepts for which the inner-product between the corresponding concept vector and any of the remaining concept vectors is larger than 0.95.

<sup>6</sup>For instance, if an OOD detector makes decisions based on outputs from an intermediate layer  $\ell$ , the user can explain it using concepts that can reconstruct the feature representations from layer  $\ell$ , or an earlier layer.

## 6 Conclusions and Future Work

In this work, we propose a first method (to the best of our knowledge) for providing concept-based attributions of the decision of an OOD detector based on high-level concepts derived from the internal feature representations of a (paired) DNN classifier. We quantify how accurately and sufficiently a set of concepts can describe an OOD detector’s behavior through a novel detection completeness metric. We also propose a general framework for learning concepts, that does not involve laborious human effort for concept annotations, by incorporating regularization terms to ensure the accurate reconstruction of the feature representation space based on concept scores. We propose a concept separability metric that encourages better interpretability of the learned concepts, and can be directly plugged into our concept learning objective. Our experiments with diverse OOD detectors and datasets confirms our insight that better separability in the concept space leads to better distinction between the resulting explanations for detected-ID and detected-OOD inputs (bringing more intuitive interpretations).

In future work, one could reduce the performance gap of the DNN classifier and OOD detector even further in our “two-world” view by borrowing insights from the knowledge-distillation literature to the regularization design [51, 52]. Future work could also include human-centric evaluations [53, 54] to assess how real users find our concept-based explanations, compared to OOD detector explanations generated by prior works such as feature attribution or concept-based interpretability (which mainly focus on class prediction).

## 7 Acknowledgement

We would like to thank Haizhong Zheng for his valuable comments. This work is partially supported by the National Science Foundation (NSF) Grants CCF-FMitF-1836978, SaTC-Frontiers-1804648, and CCF-2046710, and ARO grant number W911NF-17-1-0405, and DARPA-GARD problem under agreement number 885000.

## References

- [1] Dario Amodei, Chris Olah, Jacob Steinhardt, Paul Christiano, John Schulman, and Dan Mané. Concrete problems in AI safety. *arXiv preprint arXiv:1606.06565*, 2016.
- [2] Ian J Goodfellow, Jonathon Shlens, and Christian Szegedy. Explaining and harnessing adversarial examples. In *International Conference on Learning Representations*, 2015.
- [3] Khanh Xuan Nguyen and Brendan O’Connor. Posterior calibration and exploratory analysis for natural language processing models. In *EMNLP*, 2015.
- [4] Dan Hendrycks, Mantas Mazeika, and Thomas Dietterich. Deep anomaly detection with outlier exposure. In *International Conference on Learning Representations*, 2018.
- [5] Ziqian Lin, Sreya Dutta Roy, and Yixuan Li. MOOD: Multi-level out-of-distribution detection. In *Proceedings of the IEEE/CVF Conference on Computer Vision and Pattern Recognition*, pages 15313–15323, 2021.
- [6] Sina Mohseni, Mandar Pitale, JBS Yadawa, and Zhangyang Wang. Self-supervised learning for generalizable out-of-distribution detection. In *Proceedings of the AAAI Conference on Artificial Intelligence*, volume 34, pages 5216–5223, 2020.
- [7] Weitang Liu, Xiaoyun Wang, John Owens, and Yixuan Li. Energy-based out-of-distribution detection. *Advances in Neural Information Processing Systems*, 33, 2020.
- [8] Jiefeng Chen, Yixuan Li, Xi Wu, Yingyu Liang, and Somesh Jha. Atom: Robustifying out-of-distribution detection using outlier mining. In *Joint European Conference on Machine Learning and Knowledge Discovery in Databases*, pages 430–445. Springer, 2021.
- [9] Mukund Sundararajan, Ankur Taly, and Qiqi Yan. Axiomatic attribution for deep networks. In *International Conference on Machine Learning*, pages 3319–3328. PMLR, 2017.
- [10] Marco Tulio Ribeiro, Sameer Singh, and Carlos Guestrin. “ why should i trust you?” explaining the predictions of any classifier. In *Proceedings of the 22nd ACM SIGKDD international conference on knowledge discovery and data mining*, pages 1135–1144, 2016.
- [11] Julius Adebayo, Michael Muelly, Ilaria Liccardi, and Been Kim. Debugging tests for model explanations. In *NeurIPS*, 2020.
- [12] Amirata Ghorbani, James Wexler, James Y Zou, and Been Kim. Towards automatic concept-based explanations. *Advances in Neural Information Processing Systems*, 32:9277–9286, 2019.
- [13] Bolei Zhou, Yiyou Sun, David Bau, and Antonio Torralba. Interpretable basis decomposition for visual explanation. In *Proceedings of the European Conference on Computer Vision (ECCV)*, pages 119–134, 2018.
- [14] Diane Bouchacourt and Ludovic Denoyer. Educe: Explaining model decisions through unsupervised concepts extraction. *arXiv preprint arXiv:1905.11852*, 2019.

[15] Chih-Kuan Yeh, Been Kim, Sercan Arik, Chun-Liang Li, Tomas Pfister, and Pradeep Ravikumar. On completeness-aware concept-based explanations in deep neural networks. *Advances in Neural Information Processing Systems*, 33:20554–20565, 2020.

[16] Dan Hendrycks and Kevin Gimpel. A baseline for detecting misclassified and out-of-distribution examples in neural networks. *arXiv preprint arXiv:1610.02136*, 2016.

[17] Dan Hendrycks, Steven Basart, Mantas Mazeika, Mohammadreza Mostajabi, Jacob Steinhardt, and Dawn Song. Scaling out-of-distribution detection for real-world settings. *arXiv preprint arXiv:1911.11132*, 2019.

[18] Kimin Lee, Kibok Lee, Honglak Lee, and Jinwoo Shin. A simple unified framework for detecting out-of-distribution samples and adversarial attacks. *Advances in neural information processing systems*, 31, 2018.

[19] Jayaram Raghuram, Varun Chandrasekaran, Somesh Jha, and Suman Banerjee. A general framework for detecting anomalous inputs to DNN classifiers. In *International Conference on Machine Learning*, pages 8764–8775. PMLR, 2021.

[20] Been Kim, Martin Wattenberg, Justin Gilmer, Carrie Cai, James Wexler, Fernanda Viegas, et al. Interpretability beyond feature attribution: Quantitative testing with concept activation vectors (TCAV). In *International conference on machine learning*, pages 2668–2677. PMLR, 2018.

[21] Keinosuke Fukunaga. *Introduction to Statistical Pattern Recognition*, chapter 10, pages 446–451. Academic Press, 2 edition, 1990.

[22] Kevin P Murphy. *Machine Learning: A Probabilistic Perspective*, chapter 8, pages 271–274. MIT press, 2012.

[23] Geoffrey Hinton, Oriol Vinyals, and Jeff Dean. Distilling the knowledge in a neural network. *arXiv preprint arXiv:1503.02531*, 2015.

[24] Jimmy Ba and Rich Caruana. Do deep nets really need to be deep? *Advances in Neural Information Processing Systems*, 27, 2014.

[25] Guorui Zhou, Ying Fan, Rupeng Cui, Weijie Bian, Xiaoqiang Zhu, and Kun Gai. Rocket launching: A universal and efficient framework for training well-performing light net. In *Thirty-second AAAI conference on artificial intelligence*, 2018.

[26] Diederik P Kingma and Jimmy Ba. Adam: A method for stochastic optimization. *arXiv preprint arXiv:1412.6980*, 2014.

[27] Shiyu Liang, Yixuan Li, and R Srikant. Enhancing the reliability of out-of-distribution image detection in neural networks. In *International Conference on Learning Representations*, 2018.

[28] Christian Szegedy, Vincent Vanhoucke, Sergey Ioffe, Jon Shlens, and Zbigniew Wojna. Rethinking the inception architecture for computer vision. In *Proceedings of the IEEE conference on computer vision and pattern recognition*, pages 2818–2826, 2016.

[29] Yongqin Xian, Christoph H Lampert, Bernt Schiele, and Zeynep Akata. Zero-shot learning—a comprehensive evaluation of the good, the bad and the ugly. *IEEE transactions on pattern analysis and machine intelligence*, 41(9):2251–2265, 2018.

[30] Jianxiong Xiao, James Hays, Krista A Ehinger, Aude Oliva, and Antonio Torralba. Sun database: Large-scale scene recognition from abbey to zoo. In *2010 IEEE computer society conference on computer vision and pattern recognition*, pages 3485–3492. IEEE, 2010.

[31] Tsung-Yi Lin, Michael Maire, Serge J. Belongie, James Hays, Pietro Perona, Deva Ramanan, Piotr Dollár, and C. Lawrence Zitnick. Microsoft COCO: Common objects in context. In *European Conference on Computer Vision - ECCV*, volume 8693 of *Lecture Notes in Computer Science*, pages 740–755. Springer, 2014.

[32] Rui Huang and Yixuan Li. MOS: Towards scaling out-of-distribution detection for large semantic space. In *Proceedings of the IEEE/CVF Conference on Computer Vision and Pattern Recognition (CVPR)*, pages 8710–8719, June 2021.

[33] Bolei Zhou, Agata Lapedriza, Aditya Khosla, Aude Oliva, and Antonio Torralba. Places: A 10 million image database for scene recognition. *IEEE transactions on pattern analysis and machine intelligence*, 40(6):1452–1464, 2017.

[34] Mircea Cimpoi, Subhransu Maji, Iasonas Kokkinos, Sammy Mohamed, and Andrea Vedaldi. Describing textures in the wild. In *Proceedings of the IEEE Conference on Computer Vision and Pattern Recognition*, pages 3606–3613, 2014.

[35] Grant Van Horn, Oisin Mac Aodha, Yang Song, Yin Cui, Chen Sun, Alex Shepard, Hartwig Adam, Pietro Perona, and Serge Belongie. The INaturalist species classification and detection dataset. In *Proceedings of the IEEE conference on computer vision and pattern recognition*, pages 8769–8778, 2018.

[36] LS Shapley. A value for n-person games. *Contributions to the Theory of Games*, (28):307–317, 1953.

[37] Katsushige Fujimoto, Ivan Kojadinovic, and Jean-Luc Marichal. Axiomatic characterizations of probabilistic and cardinal-probabilistic interaction indices. *Games and Economic Behavior*, 55(1):72–99, 2006.

[38] Jianbo Chen, Le Song, Martin J Wainwright, and Michael I Jordan. L-shapley and c-shapley: Efficient model interpretation for structured data. In *International Conference on Learning Representations*, 2018.

[39] Scott M Lundberg and Su-In Lee. A unified approach to interpreting model predictions. In *Proceedings of the 31st international conference on neural information processing systems*, pages 4768–4777, 2017.

[40] Mukund Sundararajan and Amir Najmi. The many shapley values for model explanation. In *International Conference on Machine Learning*, pages 9269–9278. PMLR, 2020.

- [41] Terrance DeVries and Graham W Taylor. Learning confidence for out-of-distribution detection in neural networks. *arXiv preprint arXiv:1802.04865*, 2018.
- [42] Kimin Lee, Honglak Lee, Kibok Lee, and Jinwoo Shin. Training confidence-calibrated classifiers for detecting out-of-distribution samples. In *International Conference on Learning Representations*, 2018.
- [43] David Baehrens, Timon Schroeter, Stefan Harmeling, Motoaki Kawanabe, Katja Hansen, and Klaus-Robert Müller. How to explain individual classification decisions. *arXiv preprint arXiv:0912.1128*, 2009.
- [44] Karen Simonyan, Andrea Vedaldi, and Andrew Zisserman. Deep inside convolutional networks: Visualising image classification models and saliency maps. *arXiv preprint arXiv:1312.6034*, 2013.
- [45] Daniel Smilkov, Nikhil Thorat, Been Kim, Fernanda Viégas, and Martin Wattenberg. Smoothgrad: removing noise by adding noise. *arXiv preprint arXiv:1706.03825*, 2017.
- [46] Amirata Ghorbani, Abubakar Abid, and James Zou. Interpretation of neural networks is fragile. In *Proceedings of the AAAI Conference on Artificial Intelligence*, volume 33, pages 3681–3688, 2019.
- [47] Juyeon Heo, Sunghwan Joo, and Taesup Moon. Fooling neural network interpretations via adversarial model manipulation. *Advances in Neural Information Processing Systems*, 32:2925–2936, 2019.
- [48] Dylan Slack, Sophie Hilgard, Emily Jia, Sameer Singh, and Himabindu Lakkaraju. Fooling LIME and SHAP: Adversarial attacks on post hoc explanation methods. In *Proceedings of the AAAI/ACM Conference on AI, Ethics, and Society*, pages 180–186, 2020.
- [49] Sharon Lee Armstrong, Lila R Gleitman, and Henry Gleitman. What some concepts might not be. *Cognition*, 13(3):263–308, 1983.
- [50] Joshua Brett Tenenbaum. *A Bayesian framework for concept learning*. PhD thesis, Massachusetts Institute of Technology, 1999.
- [51] Adriana Romero, Nicolas Ballas, Samira Ebrahimi Kahou, Antoine Chassang, Carlo Gatta, and Yoshua Bengio. Fitnets: Hints for thin deep nets. *arXiv preprint arXiv:1412.6550*, 2014.
- [52] Sergey Zagoruyko and Nikos Komodakis. Paying more attention to attention: Improving the performance of convolutional neural networks via attention transfer. *arXiv preprint arXiv:1612.03928*, 2016.
- [53] Finale Doshi-Velez and Been Kim. Towards a rigorous science of interpretable machine learning. *arXiv preprint arXiv:1702.08608*, 2017.
- [54] Forough Poursabzi-Sangdeh, Daniel G Goldstein, Jake M Hofman, Jennifer Wortman Vaughan, and Hanna Wallach. Manipulating and measuring model interpretability. In *Proceedings of the 2021 CHI Conference on Human Factors in Computing Systems*, pages 1–52, 2021.
- [55] Anil Bhattacharyya. On a measure of divergence between two statistical populations defined by their probability distributions. *Bull. Calcutta Math. Soc.*, 35:99–109, 1943.
- [56] Keinosuke Fukunaga. *Introduction to Statistical Pattern Recognition*, chapter 3, pages 97–103. Academic Press, 2 edition, 1990.

## A Concept Learning

### A.1 Connection to the Bhattacharya Distance

We note that the separability metric in Eq. (7) is closely related to the Bhattacharya distance [55] for the special case when the concept scores from both ID and OOD data follow a multivariate Gaussian density. The Bhattacharya distance is a well known measure of divergence between two probability distributions, and it has the nice property of being an upper bound to the Bayes error rate in the two-class case [56]. For the special case when the concept scores from both ID and OOD data follow a multivariate Gaussian with a shared covariance matrix, it can be shown that the Bhattacharya distance reduces to the separability metric in Eq. (7) (ignoring scale factors).

### A.2 Per-class Detection Completeness

**Definition 3.** Given a trained DNN classifier  $\mathbf{f} = \mathbf{h} \circ \phi$ , a trained OOD detector with score function  $S(\mathbf{x}, \mathbf{f})$ , and a set of concept vectors  $\mathbf{C}$ , the *detection completeness* relative to class  $j \in [L]$  with respect to the ID distribution  $P_{\text{in}}(\mathbf{x}, y)$  and OOD distribution  $P_{\text{out}}(\mathbf{x})$  is defined as

$$\eta_{\mathbf{f}, S}^j(\mathbf{C}) := \frac{\sup_{\mathbf{g}} \text{AUC}^j(\mathbf{h} \circ \hat{\phi}_{\mathbf{g}, \mathbf{C}}) - b_r}{\text{AUC}(\mathbf{h} \circ \phi) - b_r}, \quad (15)$$

where  $\text{AUC}^j(\mathbf{h} \circ \hat{\phi}_{\mathbf{g}, \mathbf{C}})$  is the AUROC of the detector conditioned on the event that the class predicted by the concept-world classifier  $\mathbf{h} \circ \hat{\phi}_{\mathbf{g}, \mathbf{C}}$  is  $j$  (note that the denominator has the global AUROC). The baseline AUROC  $b_r$  is equal to 0.5 as before. This per-class detection completeness is used in the modified Shapley value defined in section 4.4.

### A.3 Per-class Concept Separability

In section 3.2, we focused on the separability between the concept scores of ID and OOD data without considering the class prediction of the classifier. However, it would be more appropriate to impose a high separability between the concept scores on a per-class level. In other words, we would like the concept scores of detected-ID and detected-OOD data, that are predicted by the classifier into any given class  $y \in [L]$  to be well separated. Consider the set of concept-score vectors from the detected-ID (or detected-OOD) dataset that are also predicted into class  $y$ :

$$\begin{aligned} V_{\text{in}}^y(\mathbf{C}) &:= \{\tilde{\mathbf{v}}_{\mathbf{C}}(\mathbf{x}), \mathbf{x} \in D_{\text{in}}^{\text{tr}} \cup D_{\text{out}}^{\text{tr}} : \mathcal{D}_{\gamma}(\mathbf{x}, \mathbf{f}) = 1 \text{ and } \hat{y}(\mathbf{x}) = y\} \\ V_{\text{out}}^y(\mathbf{C}) &:= \{\tilde{\mathbf{v}}_{\mathbf{C}}(\mathbf{x}), \mathbf{x} \in D_{\text{in}}^{\text{tr}} \cup D_{\text{out}}^{\text{tr}} : \mathcal{D}_{\gamma}(\mathbf{x}, \mathbf{f}) = 0 \text{ and } \hat{y}(\mathbf{x}) = y\}. \end{aligned} \quad (16)$$

We can extend the definition of the global separability metric in Eq. (7) to a given predicted class  $y \in [L]$  as follows

$$\begin{aligned} J_{\text{sep}}^y(\mathbf{C}) &:= J_{\text{sep}}(V_{\text{in}}^y(\mathbf{C}), V_{\text{out}}^y(\mathbf{C})) = \text{tr}[(\mathbf{S}_w^y)^{-1} \mathbf{S}_b^y] \\ &= (\boldsymbol{\mu}_{\text{out}}^y - \boldsymbol{\mu}_{\text{in}}^y)^T (\mathbf{S}_w^y)^{-1} (\boldsymbol{\mu}_{\text{out}}^y - \boldsymbol{\mu}_{\text{in}}^y). \end{aligned} \quad (17)$$

The scatter matrices  $\mathbf{S}_w^y$  and  $\mathbf{S}_b^y$  are defined similar to Eq. (5), using the per-class subset of concept scores  $V_{\text{in}}^y(\mathbf{C})$  or  $V_{\text{out}}^y(\mathbf{C})$ , and the mean concept-score vectors from the detected-ID and detected-OOD dataset are also defined at a per-class level.

### A.4 Algorithm for Concept Learning

To provide the readers with a clear overview of the proposed concept learning approach, we include Algorithm 1. Note that in line 7 of Algorithm 1, the dimension reduction step in  $V_{\text{in}}(\mathbf{C}) = \{\tilde{\mathbf{v}}_{\mathbf{C}}(\mathbf{x}), \mathbf{x} \in D_{\text{in}}^{\text{tr}} \cup D_{\text{out}}^{\text{tr}} : \mathcal{D}_{\gamma}(\mathbf{x}, \mathbf{f}) = 1\}$  and  $V_{\text{out}}(\mathbf{C}) = \{\tilde{\mathbf{v}}_{\mathbf{C}}(\mathbf{x}), \mathbf{x} \in D_{\text{in}}^{\text{tr}} \cup D_{\text{out}}^{\text{tr}} : \mathcal{D}_{\gamma}(\mathbf{x}, \mathbf{f}) = 0\}$  involves the maximum function, which is not differentiable; specifically, the step  $\tilde{v}_{\mathbf{c}_i}(\mathbf{x}) = \max_{p,q} |\langle \phi^{p,q}(\mathbf{x}), \mathbf{c}_i \rangle|$ . For calculating the gradients (backward pass), we use the log-sum-exp function with a temperature parameter to get a differentiable approximation of the maximum function, *i.e.*,  $\max_{p,q} |\langle \phi^{p,q}(\mathbf{x}), \mathbf{c}_i \rangle| \approx \alpha \log \left[ \sum_{p,q} \exp \left( \frac{1}{\alpha} |\langle \phi^{p,q}(\mathbf{x}), \mathbf{c}_i \rangle| \right) \right]$  as  $\alpha \rightarrow 0$ . In our experiments, we set the temperature constant  $\alpha = 0.001$  upon checking that the approximate value of  $\tilde{v}_{\mathbf{c}_i}(\mathbf{x})$  is sufficiently close to the original value using the maximum function.

### A.5 Implementation Details

In this section, we provide more details about our experiment setting.

**Algorithm 1** Learning concepts for OOD detector**INPUT:** Entire training set  $D^{\text{tr}} = \{D_{\text{in}}^{\text{tr}}, D_{\text{out}}^{\text{tr}}\}$ , entire validation set  $D^{\text{val}} = \{D_{\text{in}}^{\text{val}}, D_{\text{out}}^{\text{val}}\}$ , classifier  $f$ , detector  $\mathcal{D}_\gamma$ .**INITIALIZE:** Concept vectors  $\mathbf{C} = [\mathbf{c}_1 \dots \mathbf{c}_m]$  and parameters of the network  $g$ .**OUTPUT:**  $\mathbf{C}$  and  $g$ .

- 1: Calculate threshold  $\gamma$  for  $\mathcal{D}_\gamma$  using  $D^{\text{val}}$  as the score at which true positive rate is 95%.
- 2: **for**  $t = 1, \dots, T$  epochs **do**
- 3:   Compute the prediction accuracy of the concept-world classifier  $\mathbf{f}^{\text{con}}$  using  $D_{\text{in}}^{\text{tr}}$ .
- 4:   Compute the explainability regularization term as defined in [15].
- 5:   Compute difference of feature representation between canonical world and concept world using Eqn. (10).
- 6:   Compute difference of detector outputs between canonical world and concept world using Eqn. (11).
- 7:   Compute  $V_{\text{in}}(\mathbf{C})$  and  $V_{\text{out}}(\mathbf{C})$  using  $D^{\text{tr}}$ ,  $\mathcal{D}_\gamma$  and  $\mathbf{C}$ .
- 8:   Compute separability between  $V_{\text{in}}(\mathbf{C})$  and  $V_{\text{out}}(\mathbf{C})$  using Eqn. (7) or Eqn. (17).
- 9:   Perform a batch-SGD update of  $\mathbf{C}$  and  $g$  using Eqn. (12) as the objective.
- 10: **end for**

**OOD Datasets.** For the auxiliary OOD dataset for concept learning ( $D_{\text{out}}^{\text{tr}}$ ), we use the unlabeled images from MSCOCO dataset (120K images in total) [31]. We carefully curate the dataset to make sure that no images contain overlapping animal objects with our ID dataset (*i.e.*, 50 animal classes of Animals-with-Attributes [29]), then randomly sample 30K images. For OOD datasets for evaluation ( $D_{\text{out}}^{\text{te}}$ ), we use the high-resolution image datasets processed by Huang and Li [32].

**Hyperparameters.** Throughout the experiments, we fix the number of concepts to  $m = 100$  (unless specifically mentioned otherwise), and following the implementation of [15], we set  $\lambda_{\text{expl}} = 10$  and  $g$  to be a two-layer fully-connected neural network with 500 neurons in the hidden layer. We learn concepts based on feature representations from the layer right before the global max-pooling layer of the Inception-V3 model. We set the range of  $\lambda_{\text{norm}}$ ,  $\lambda_{\text{mse}}$  and  $\lambda_{\text{sep}}$  (in Eqn. (12)) based on the scale of corresponding regularization terms (*i.e.*,  $J_{\text{norm}}(\mathbf{C}, g)$ ,  $J_{\text{mse}}(\mathbf{C}, g)$  and  $J_{\text{sep}}(\mathbf{C})$ , respectively), for a specific choice of the OOD detector. After concept learning with  $m$  concepts, we remove any duplicate (redundant) concept vectors by removing those with a dot product larger than 0.95 with the remaining concept vectors [15].

## A.6 Additional Results

### Ablation study for concept learning.

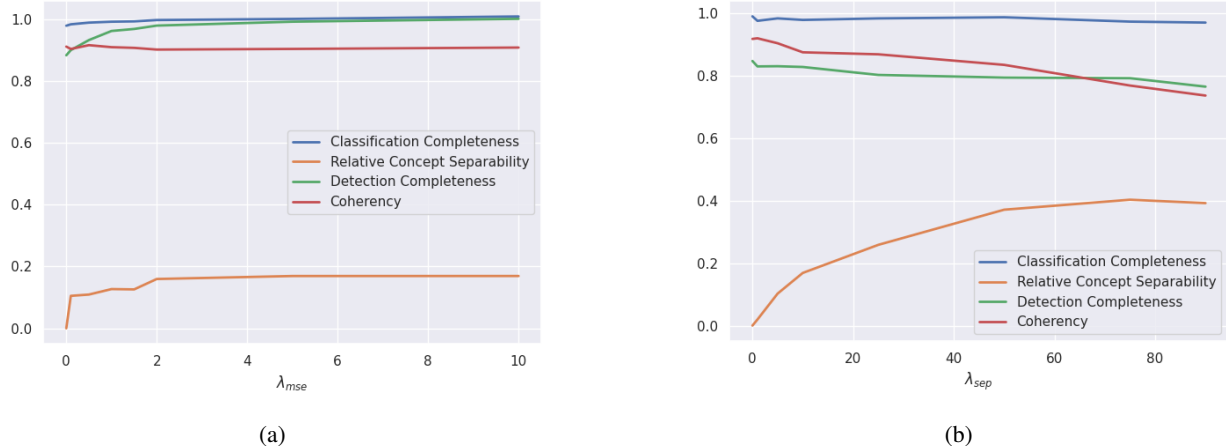


Figure 6: **Ablation study with respect to  $J_{\text{mse}}(\mathbf{C}, g)$  and  $J_{\text{sep}}(\mathbf{C})$ .** We fix  $m = 100$ ,  $\lambda_{\text{expl}} = 10$ , and the OOD detector used for concept learning and evaluation is Energy [7]. For (a), we set  $\lambda_{\text{norm}} = 0.1$ ,  $\lambda_{\text{sep}} = 0$ , and for (b),  $\lambda_{\text{mse}} = 0$ ,  $\lambda_{\text{norm}} = 0$ .

We perform an ablation study that isolates the effect of each regularization term in our concept learning objective (Eqn. 12) towards our evaluation metrics: classification completeness, detection completeness, and relative concept separability. We also observe the coherency among the learned concepts by varying  $\lambda_{\text{mse}}$  and  $\lambda_{\text{sep}}$ . Coherency of concepts was introduced by Ghorbani *et al.* [12] to ensure that the generated concept-based explanations are understandable to

humans. It captures the idea that the examples for a concept should be similar to each other, while being different from the examples corresponding to other concepts. For the specific case of the image domain, the receptive fields most correlated to a concept  $i$  (e.g., "stripe pattern") should look different from the receptive fields for a different concept  $j$  (e.g., "wavy surface of sea"). Yeh *et al.* [15] proposed to quantify the coherency of concepts as

$$\frac{1}{mK} \sum_{i=1}^m \sum_{\mathbf{x}' \in T_{\mathbf{c}_i}} \langle \phi(\mathbf{x}'), \mathbf{c}_i \rangle, \quad (18)$$

where  $T_{\mathbf{c}_i}$  is the set of  $K$ -nearest neighbor patches of the concept vector  $\mathbf{c}_i$  from the ID training set  $D_{\text{in}}^{\text{tr}}$ . We use this metric to quantify how understandable our concepts are for different hyperparameter choices. Figure 6a shows that aligned with our intuition, large  $\lambda_{\text{mse}}$  helps to improve the detection completeness. Having non-zero  $\lambda_{\text{mse}}$  is also helpful to improve the classification completeness even further, and surprisingly concept separability as well, without sacrificing the coherency of concepts. On the other hand, in Figure 6b, we observe that large relative concept separability with large  $\lambda_{\text{sep}}$  comes at the expense of lower detection completeness and coherency. Recall that when visualizing what each concept represents for human's convenience, we apply threshold 0.8 to only presents (see Figure 7). Low coherency with respect to Eqn. 18 (i.e., 0.768 with  $\lambda_{\text{sep}} = 75$ ) means that there are much less number of examples that can pass the threshold, meaning that users can hardly understand what the concepts at hand entails. This observation suggests that one needs to balance between concept coherency and concept separability depending on which property would be more useful for a specific application of concepts.

**Transferability of concepts across OOD detectors.** Our work essentially suggests to use different set of concepts for a specific target OOD detector, as  $J_{\text{mse}}(\mathbf{C}, \mathbf{g})$  and  $J_{\text{sep}}(\mathbf{C})$  in Eqn. (12) depend on a choice of OOD detector. In practice, however, one might not have enough computational capacity to prepare multiple sets of concepts for all type of OOD detectors at hand. Here, we inspect whether the concepts targeted for a certain type of OOD detector are also good to be used for other OOD detectors.

We explore the transferability of concepts targeted to MSP [16] detector in Table 2, and Energy [7] in Table 3. Not surprisingly, we observe that concepts targeted for Energy yields the best detection completeness score when tested with the same type of OOD detector, but still make meaningful improvement with other detectors as well. When it comes to relative concept separability, it is transferred even better across different OOD detectors. For instance, the concepts lead to  $J_{\text{sep}}(\mathbf{C}, \mathbf{C}') = 0.862$  with Textures, the best relative concept separability is achieved with ODIN detector (i.e.,  $J_{\text{sep}}(\mathbf{C}, \mathbf{C}') = 0.862$ ) and which is even higher than the best results we could obtain using the set of concepts targeted for ODIN (i.e.,  $J_{\text{sep}}(\mathbf{C}, \mathbf{C}') = 0.414$  with  $\lambda_{\text{mse}} = 0, \lambda_{\text{norm}} = 0, \lambda_{\text{sep}} = 50$  in Table 1).

OOD dataset	Metrics	$\mathcal{D}$			
		MSP	ODIN	Energy	Mahal
Places	$\eta_{\mathbf{f},S}(\mathbf{C})$	0.959	0.952	0.938	0.947
	$J_{\text{sep}}(\mathbf{C}, \mathbf{C}')$	0.327	0.288	0.361	0.338
SUN	$\eta_{\mathbf{f},S}(\mathbf{C})$	0.961	0.954	0.945	0.953
	$J_{\text{sep}}(\mathbf{C}, \mathbf{C}')$	0.266	0.294	0.390	0.351
Textures	$\eta_{\mathbf{f},S}(\mathbf{C})$	0.938	0.946	0.932	0.930
	$J_{\text{sep}}(\mathbf{C}, \mathbf{C}')$	0.344	0.279	0.313	0.335
iNaturalist	$\eta_{\mathbf{f},S}(\mathbf{C})$	0.946	0.946	0.933	0.930
	$J_{\text{sep}}(\mathbf{C}, \mathbf{C}')$	0.286	0.181	0.229	0.197

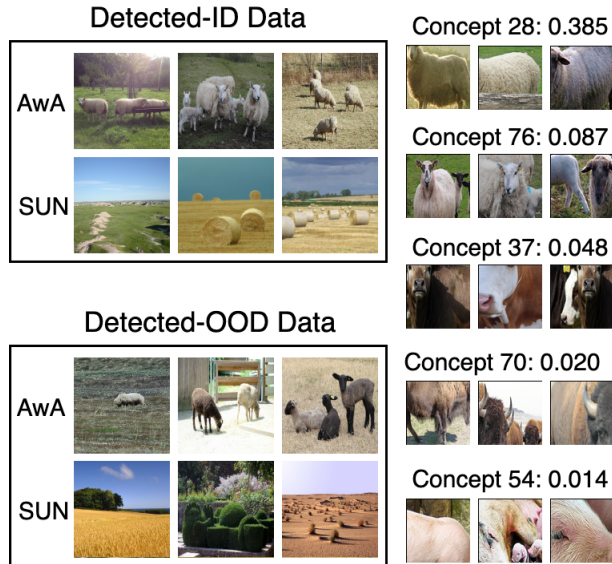
Table 2: **Transferability of concepts targeted for MSP with  $\lambda_{\text{mse}} = 10, \lambda_{\text{norm}} = 0.1, \lambda_{\text{sep}} = 50$**

## B Explanations

### B.1 Important concepts for each OOD detector

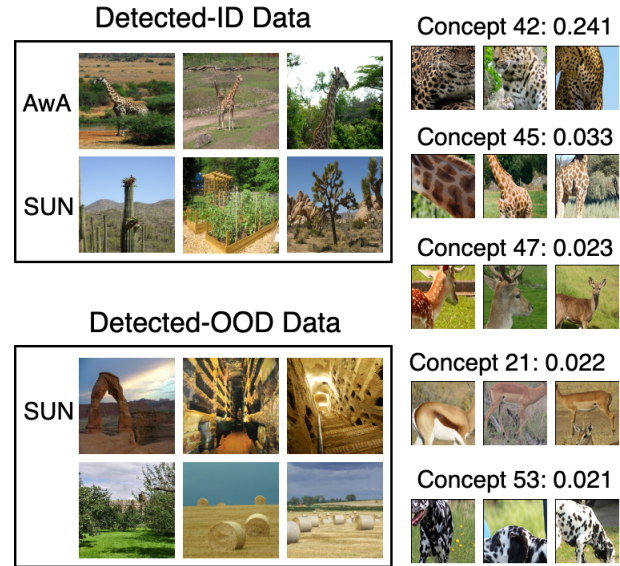
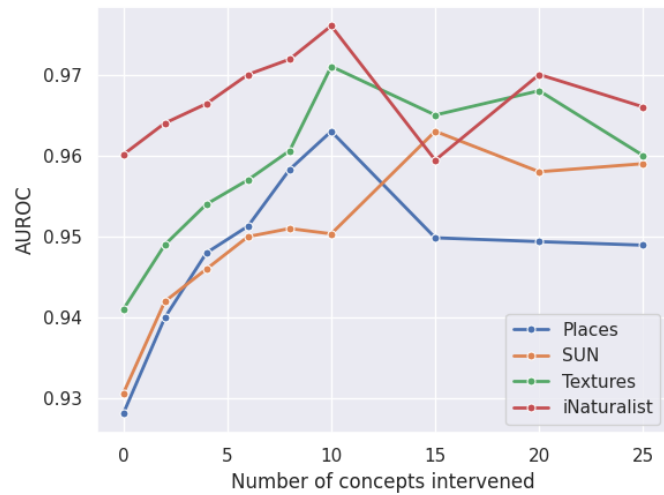
We show additional examples for the top-ranked concepts by SHAP( $\eta_{\mathbf{f},S}, \mathbf{c}_i$ ) in Figure 8. For each figure with a fixed choice of class prediction, we present receptive fields from ID test set corresponding to top concepts that contribute the most to the decisions of each OOD detector. All receptive fields passed the threshold test that the inner product between the feature representation and the corresponding concept vector is over 0.8.

OOD data	Metrics	OOD detector			
		MSP	ODIN	Energy	Mahal
Places	$\eta_{f,S}(C)$	0.956	0.954	0.971	0.954
	$J_{sep}(C, C')$	0.417	0.415	0.365	0.410
SUN	$\eta_{f,S}(C)$	0.949	0.948	0.970	0.950
	$J_{sep}(C, C')$	0.355	0.286	0.400	0.353
Textures	$\eta_{f,S}(C)$	0.931	0.943	0.964	0.947
	$J_{sep}(C, C')$	0.567	0.862	0.494	0.701
iNaturalist	$\eta_{f,S}(C)$	0.943	0.939	0.973	0.940
	$J_{sep}(C, C')$	0.283	0.448	0.280	0.326

Table 3: **Transferability of concepts targeted for Energy with**  $\lambda_{mse} = 1$ ,  $\lambda_{norm} = 0.1$ ,  $\lambda_{sep} = 50$ .Figure 7: **Top-6 important concepts for Energy with respect to class "Sheep".**

## B.2 Counterfactual analysis

To verify the important concepts identified by our modified Shapley value, we perform counterfactual analysis, addressing the following question: *if the OOD detector thought the input has different score for this concept, would the detection result be different?* As we do not assume to have groundtruth annotation for concepts, we construct concept score profiles of detected-ID (or detected-OOD) inputs from held-out ID (or OOD) dataset, and refer to this as ID (or OOD) concept profile. With the guidance of ID and OOD concept profiles, we take intervention on the concept scores of mis-detected inputs. Specifically, for ID data mis-detected as OOD, we update their concept scores using ID profiles, and similarly, for OOD data mis-detected as ID, their concept scores are updated with OOD profiles. The number of concepts to be intervened can be varied. As shown in Figure 9, with intervention on more number of important concepts (ranked by  $SHAP(\eta_{f,S}, c_i)$ ), we observe an improved performance of OOD detector in concept world.


 Figure 8: **Top-6 important concepts for Energy with respect to class "Giraffe"**

 Figure 9: **Performance of MSP with test-time interventions on concept scores.**